

Simple strong glass forming models: mean-field solution with activation

Arnaud Buhot^{1,2*}, Juan P. Garrahan^{1†} and David Sherrington^{1‡}

¹*Theoretical Physics, University of Oxford, 1 Keble Road, Oxford, OX1 3NP, U.K.*

²*CEA Grenoble, DRFMC, SI3M, 17 rue des Martyrs, 38054 Grenoble, France.*

(February 1, 2008)

We introduce simple models, inspired by previous models for froths and covalent glasses, with trivial equilibrium properties but dynamical behaviour characteristic of strong glass forming systems. These models are also a generalization of backgammon or urn models to a non-constant number of particles, where entropic barriers are replaced by energy barriers, allowing for the existence of activated processes. We formulate a mean-field version of the models, which keeps most of the features of the finite dimensional ones, and solve analytically the out-of-equilibrium dynamics in the low temperature regime where activation plays an essential role.

PACS numbers: 64.70.Pf, 61.20.Lc., 05.70.Ln

I. INTRODUCTION

Glass forming systems, like supercooled liquids, display remarkable dynamical properties, and are the subject of intense experimental and theoretical studies (for reviews see [1–3]). Out of all glass formers, the ones which have the seemingly simpler macroscopic behaviour are strong liquids, typically covalently bonded systems like SiO₂ and GeO₂, in which viscosities and relaxation times increase exponentially with decreasing temperature, following a simple Arrhenius law [1]. While the increase of timescales in strong systems is not as dramatic as in fragile ones, it is still very pronounced, and, moreover, it is not accompanied by the growth of static lengthscales or similar corresponding structural signatures.

The separation of statics and dynamics is a central feature of structural glass formers [4], and is in marked contrast with other dynamically arrested systems, like spin glasses and other systems with quenched disorder [5,6]. This leads naturally to an approach for modeling these systems based on the idea that glassiness is not a consequence of disorder or frustration in the static interactions but of constraints on their dynamics [7–10]. The aim of this paper is to build on our earlier efforts in the modeling of covalent systems and froths [11–13], where the dynamical constraints that lead to glassy slowdown can be related directly to elementary structural processes, and develop a class of models which retain the essential features but are simple enough to allow for analytical solutions, and study in detail the connection with underlying effective diffusion-annihilation processes [14,15] which we believe are an essential component of strong glass formers in general.

The models we study in this work are described explicitly and concisely in section II. Here we outline briefly the background considerations which were their conceptual basis. They are a distillation of a series of minimalist models exhibiting strong glass-like dynamical behaviour through the operation of kinetic constraints despite non-interacting Hamiltonians and trivial thermodynamics (with no equilibrium phase transitions) and no imposed quenched disorder.

The first model [11] was a 2-dimensional topological ‘foam’ consisting of a fully pairwise connected network of three-armed vertices with energy function $E = \sum_i (n_i - 6)^2$ where n_i is the number of edges (sides) of cell i ; thus it emulates desire for local hexagonal structure without the complication of interaction. The dynamics is $T1$ (see Fig. 1) performed stochastically with acceptance probabilities determined by the Boltzmann ratio $\exp(-\Delta E/T)$ where ΔE is the resultant energy change and T is the temperature. This ensures eventual equilibration at any finite temperature but also provides a kinetic constraint since each $T1$ move involves four cells, decreases n by 1 for each of the two initially adjacent cells and increases n of the other two by the same amount.

*Email: buhot@drfmc.ceng.cea.fr.

†Email: j.garrahan1@physics.ox.ac.uk.

‡Email: d.sherrington1@physics.ox.ac.uk.

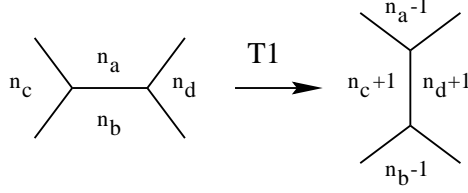


FIG. 1. A $T1$ move. The initially adjacent cells decrease their number of neighbours by 1 whereas the cells which become adjacent increase their number of neighbours by 1.

This model can be considered variously as an idealization of a glass of covalent sp^2 hybrid bonds which change connections, or of the Voronoi cells surrounding a fluid of atoms, or of a foam ; in the first case effectively allowing for harmonic changes of vertex angle energy but ignoring cell-cell correlation energies, in the second and third replacing continuous energies associated with interatomic forces or surface tension by the simple topological energies. At low temperatures the model exhibits two-timescale macro-behaviour, for example in the decay of the energy from a random start or in the autocorrelation function even in equilibrium. The fast timescale is temperature independent and the slow timescale is Arrhenius-like: $\tau \sim \exp(a/T)$, $a \simeq 2$ [11,12]. This behaviour can be understood by considering $n_i = 6$ as ‘perfect’ and $n_i \neq 6$ as ‘defect’ cells, and the cooperative behaviour in terms of the diffusion and annihilation of defects. The fast processes correspond to ones which involve either an energy decrease or no energy change, while the slow processes involve energetic defect creation. Defects with $|n_i - 6| > 1$ disappear rapidly at low temperature so we concentrate on $|n_i - 6| \leq 1$. Let us denote $n = 5(7)$ cells by $A(\bar{A})$ and $n = 6$ by \emptyset . Then energy reduction is due to the annihilation of an $A\bar{A}$ neighbouring pair (or dimer). The $T1$ process however involves four cells and only allows $A\bar{A}$ dimer annihilation if at most only one of the other cells involved is a \emptyset ; thus the annihilation of two dimers [16]

$$2A + 2\bar{A} \rightarrow 4\emptyset \quad (1)$$

exists as well as the single dimer annihilation [17]

$$2A + \bar{A} + \emptyset \rightarrow 3\emptyset + A, \quad 2\bar{A} + A + \emptyset \rightarrow 3\emptyset + \bar{A}. \quad (2)$$

$A\bar{A}$ dimers can diffuse on the fast (microscopic attempt) timescale if the other pair of cells in the $T1$ process are both \emptyset :

$$A + \bar{A} + 2\emptyset \rightarrow 2\emptyset + A + \bar{A}. \quad (3)$$

Defects are only annihilated in dimer pairs ($A\bar{A}$) and isolated defects must be paired to annihilate, hence they must be moved together. However they can only move via processes which involve the creation of an $A\bar{A}$ dimer and a consequent energetic penalty; i.e. by the inverses of processes (2)

$$A + 3\emptyset \rightarrow \emptyset + 2A + \bar{A}, \quad \bar{A} + 3\emptyset \rightarrow \emptyset + 2\bar{A} + A, \quad (4)$$

which are slower by the Boltzmann factor $\exp(-2/T)$. Dimer pairs, of either of the two possible $A\bar{A}$ combinations on the right hand sides of processes (4) can then diffuse away freely by process (3). Processes (2) themselves also allow slow movement of A (or \bar{A}) via collision with a roaming $A\bar{A}$ dimer, leading to annihilation of all three A, \bar{A} but creation of A (or \bar{A}) on the cell which was originally \emptyset . This also involves a slowing factor $\exp(-2/T)$ since the equilibrium density of $A\bar{A}$ dimers involves such a factor. As a consequence, at low temperatures, the energy after a quench from a random/high temperature start quickly decays to a plateau through elimination of $A\bar{A}$ dimers, leaving mainly (and at $T = 0$ only) isolated defects and clusters of only like defects. After this plateau, the energy further decays to equilibrium with the Arrhenius-like timescale $\tau \sim \exp(a/T)$ due to the effective dimer-mediated diffusion of isolated defects and eventual $A\bar{A}$ pairing and annihilation.

The second generation of models is built on the above picture, replacing the foam by lattice-based models with ‘spins’ associated with the dual plaquettes [18]

$$S_i = 1, 0, -1, \quad (5)$$

the energy by

$$E = J \sum_{i=1}^N S_i^2, \quad (6)$$

and the $T1$ move by one involving four spins around a corresponding ‘Feynman diagram’ edge in a hexagonal lattice, a square vertex in a square lattice, etc. [13]. For $J > 0$ this behaves essentially as for the foam model [19], but allows much larger simulations. The resultant better-accuracy data permits comparison with the asymptotic predictions of the field theory of simple diffusion–annihilation processes [14,15] of type $A + B \rightarrow \emptyset$ (in the usual notation of that subject); the agreement is quite good for both decays which can be viewed as diffusion–annihilation processes with different timescales [13].

The second class of models permits a further modification, the taking of $J < 0$. In this case the ground state is highly degenerate ($S_i = \pm 1$ independently on each plaquette), as compared with the unique ground state for $J > 0$ ($S_i = 0$; all i), but the defects are of only one type ($S_i = 0$). The two timescale behaviour of the energy decay to equilibrium and of the equilibrium autocorrelation functions persists. Ignoring the complications of the ground state degeneracy and further constraints imposed by the $T1$ process ($|S_i|$ cannot be increased above 1) the behaviour is now describable in terms of only A , \emptyset dynamics (the \emptyset now referring to $S = \pm 1$ and A to $S = 0$). The qualitative discussion earlier still applies with \bar{A} (or B) replaced by A . Again the comparison with the predictions of simple field theory of diffusion–annihilation is fair, but less precise, presumably in part due to the more complicated ground state degeneracy and constraints.

The models studied in this paper are a further simplification which maintain the features of (i) fast annihilation of dimers, (ii) fast diffusion of dimers, (iii) motion of isolated defects only by slow creation of dimers. It allows for either a single defect type (A) and identical-defect dimers (AA) or two defect types (A and B) and mixed dimers (AB), but in both cases with a non-degenerate ($T = 0$ absorbing) ground state (\emptyset). They also allow separation of the timescales for processes (i) and (ii) above, as well as their separation from (iii). The explicit formulation is given in the next section, but the above should clarify why they are appropriate.

The rest of the paper is organized as follows. In section II we give a full description of the models studied in this work. Their general features are discussed and compared with those of previous models in section III. In section IV we solve analytically the mean-field version of the models. Our conclusions are given in section V. Details of the analytical calculations are provided in the appendices.

II. DESCRIPTION OF THE MODELS

The minimalist models we study here are based on a coarse-grained simplification of the ideas described above. They correspond to defects (or particles), which can be either of a single kind A , or different kinds, A and B , and live in a d dimensional lattice. They can also be considered as a generalization of backgammon [21] or urn models [22] to a non-constant number of particles, with energetic barriers rather than entropic ones, thus allowing for the existence of activated processes. The analogy with previous models [11–13] is obtained through the dynamical rules which mimic the different processes (2), (3) and (4). The two models under consideration are the following.

A. Single type of particles

As for previous models, with each defect (particle in our case) we associate a unit energy ($J = 1$) leading to the Hamiltonian

$$H = \sum_{i=1}^N n_i, \quad (7)$$

with n_i the occupation number on site i . Due to the non-interacting Hamiltonian, the equilibrium properties are trivial. The probabilities p_n^{eq} to have n particles on a given site at temperature $T = 1/\beta$ are:

$$p_n^{eq}(\beta) = e^{-\beta n} \left(\sum_{n=0}^{n_{\max}} e^{-\beta n} \right)^{-1} \quad (8)$$

and lead to an equilibrium energy or concentration of particles:

$$c_{eq}(\beta) = \sum_{n=0}^{n_{\max}} n p_n^{eq}(\beta) \quad (9)$$

with n_{\max} the maximum number of particles per site. In the following we use the smallest number ($n_{\max} = 3$) compatible with the dynamical rules. The infinite temperature concentration $c_{eq}(\beta = 0) = 3/2$ corresponds to equal probabilities $p_n^{eq} = 1/4$ whereas the low temperature concentration vanishes as $c_{eq}(\beta) \sim e^{-\beta}$.

The dynamical rules are inspired from the $T1$ moves [11–13]. Three different kinds of moves are considered [20]:

(i) The annihilation of two particles analogous to processes (2): three particles disappear from site i and only one appears on a neighbouring site j with a rate 1

$$(n_i, n_j) \rightarrow (n_i - 3, n_j + 1) \quad (10)$$

(ii) The dimer diffusion analogous to process (3): two particles move from site i to a neighbouring site j with a diffusive rate D

$$(n_i, n_j) \rightarrow (n_i - 2, n_j + 2) \quad (11)$$

(iii) The creation of two particles analogous to processes (4): a particle disappears from site i to create three particles on a neighboring site j with a rate $e^{-2\beta}$

$$(n_i, n_j) \rightarrow (n_i - 1, n_j + 3) \quad (12)$$

Those moves have also to respect the maximal number of particles per site $n_{\max} = 3$. The rates considered satisfy detailed balance with respect to Hamiltonian (7), ensuring that the equilibrium properties [equations (8) and (9)] will be reached asymptotically by the dynamics. All these processes are of the form $(n_i, n_j) \rightarrow (n_i - x, n_j + y)$ with $x + y = 4$, which reflects the four cell character of the original model transitions.

The introduction of a diffusive constant D allows to separate explicitly the timescales for diffusion of dimers from that of the annihilation process. It is also interesting to notice that those rules are defined for any dimension and any lattice, even for a fully connected network, leading the possibility to study the mean-field version of the model.

B. Two different types of particles

A possible modification of the model consists in considering two different types of particles (A and B) to keep the analogy with the possible sign of the topological charges $q_i = 6 - n_i$ of the cells in the foam model. As a consequence, the dynamical rules are closer to the $T1$ move. This modification allows to stress the relation between the last decay of the energy or concentration of particles and diffusion–annihilation processes [14,15], since the critical dimension and exponents for the $A + B \rightarrow \emptyset$ process is different from those of the $A + A \rightarrow \emptyset$ one.

The presence of two types of particles introduce modifications to the equilibrium properties. In the following we still consider a restriction on the number of particles per site ($n_{\max} = 3$) irrespective of their nature, but, in addition, the difference between the numbers of A and B particles on a site is limited to $-1, 0$ or 1 (this last restriction absent within the previous model avoids configurations with all A 's or all B 's on a given site). As a consequence the equilibrium probabilities to have n_A particles A and n_B particles B on a given site are (with $n = n_A + n_B$):

$$p_{n_A, n_B}^{eq}(\beta) = \frac{1}{Z} e^{-\beta n} \Theta(n_{\max} - n) \Theta(1 - |n_A - n_B|) \quad (13)$$

leading to the equilibrium concentration of particles:

$$c_{eq}(\beta) = \sum_{n_A, n_B} n p_{n_A, n_B}^{eq}(\beta) \quad (14)$$

with:

$$Z = \sum_{n_A, n_B} e^{-\beta n} \Theta(n_{\max} - n) \Theta(1 - |n_A - n_B|) \quad (15)$$

and $\Theta(x)$ the Heaviside function ($\Theta(x) = 1$ if $x \geq 0$ and $\Theta(x) = 0$ otherwise).

The infinite temperature concentration of particles is $c_{eq}(\beta = 0) = 5/3$ [six possible configurations with equal probabilities: $(n_A, n_B) = (0, 0), (1, 0), (0, 1), (1, 1), (2, 1)$ and $(1, 2)$] whereas for low temperatures the concentration vanishes as $c_{eq}(\beta) \sim 2e^{-\beta}$ (the coefficient 2 is coming from an entropic effect due to the two types of particles).

The dynamical rules are a straightforward generalization of the $T1$ moves [11–13]. Three different kinds of moves are considered:

(i) annihilation of an AB dimer analogous to processes (2), an AB dimer and another particle disappear from site i but only the single particle appears on a neighbouring site j with a rate 1

$$[(AAB)_i, (X)_j] \rightarrow [(\emptyset)_i, (AX)_j], \quad [(ABB)_i, (X)_j] \rightarrow [(\emptyset)_i, (BX)_j] \quad (17)$$

(ii) AB dimer diffusion analogous to process (3), a dimer moves from site i to a neighbouring site j with a diffusive rate D

$$[(ABX)_i, (Y)_j] \rightarrow [(X)_i, (ABY)_j] \quad (18)$$

(iii) creation of an AB dimer analogous to processes (4), a single particle from site i move to a neighbouring site j creating a dimer on this site with a rate $e^{-2\beta}$

$$[(AX)_i, (\emptyset)_j] \rightarrow [(X)_i, (AAB)_j], \quad [(BX)_i, (\emptyset)_j] \rightarrow [(X)_i, (ABB)_j] \quad (20)$$

In all of these processes, symbols X and Y stand for possible A , B or \emptyset particles respecting the restrictions in the number of particles on each site. The rates again satisfy detailed balance conditions, ensuring equilibration.

III. GENERAL FEATURES

We now show that the two models introduced in the last section share common behaviour for all dimensions and with the models considered previously [11–13]. In what follows we discuss equilibrium dynamical properties, in particular the existence of two different timescales, as well as out-of-equilibrium features like the multi-stage decay of the energy density after a quench.

A. Dynamics in equilibrium

Let us first consider the equilibrium dynamical properties of these systems. As we already mentioned, the dynamical behaviour is characteristic of a strong glass [1]. The relaxation time increases exponentially with the inverse temperature, corresponding to an Arrhenius law. A simple way to determine this relaxation time is from the auto-correlation function:

$$C(t, t') = \langle n_i(t) n_i(t') \rangle \quad (21)$$

with the brackets denoting ensemble average. In equilibrium this two-time function reduces to a single time equilibrium correlation $C_{eq}(t - t')$ due to the time translational invariance. We can define the relaxation time τ from $C_{eq}^c(\tau) = C_{eq}^c(0)/e$, where the connected correlation $C_{eq}^c(t) = C_{eq}(t) - c_{eq}^2$. At low temperatures and for all diffusive constants, the temperature dependent and slower process is the creation of particles which has energy barrier $\Delta E = 2$. As a consequence we expect the following Arrhenius law for the relaxation time:

$$\tau(\beta) \propto e^{2\beta}. \quad (22)$$

This behaviour is confirmed by numerical simulations. The expected Arrhenius law (22) is recovered for all dimensions and all diffusive constants (see Fig. 2). Similar results are found for the model with two types of particles. (Simulations have been performed using continuous time Monte Carlo [23] for systems of $N = 10^6$ sites.)

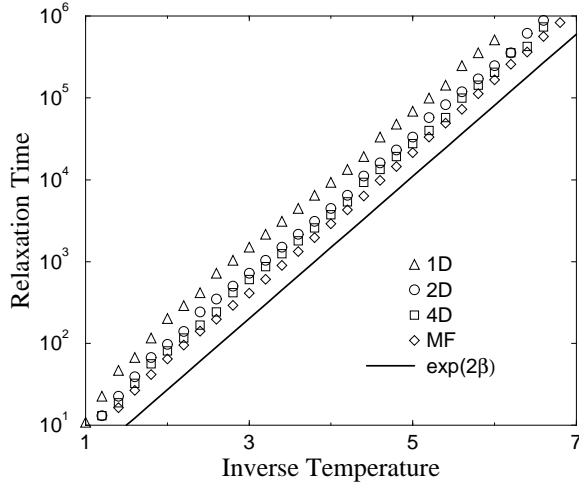


FIG. 2. Relaxation time as function of the inverse temperature for different dimensions ($d = 1, 2, 4$ and ∞) and a diffusive constant $D = 10^{-4}$. The line corresponds to the expected $\tau \propto e^{2\beta}$ behaviour.

The equilibrium correlation explicitly shows the two timescale behaviour (see Fig. 3): (i) dimer diffusion or annihilation on a short timescale independent of the temperature and (ii) isolated particle motion through the creation of a dimer on the relaxation timescale. At low temperatures when the two timescales are well separated the correlation presents a plateau separating the two relaxing decays. The relative position of this plateau is increasing with decreasing the temperature due to the fast disappearance of dimers. The decay to zero of the connected correlation is also dimension dependent. A change of behaviour occurs between the mean-field case ($d = \infty$), where it is exponential, and finite dimensions ($d = 2$ in Fig. 3), where it only vanishes algebraically. The probability for a particle to come back to the same place (which depends on the dimension of the system) explains this difference.

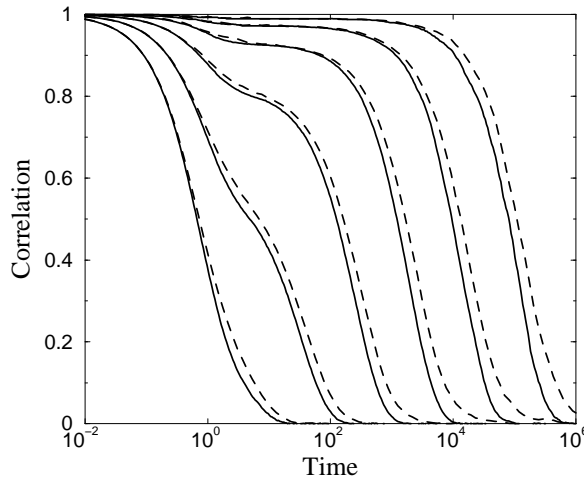


FIG. 3. Normalized equilibrium autocorrelation $C_{eq}^c(t)/C_{eq}^c(0)$ for the model with a single type of particles and a diffusive constant $D = 1$. Different temperatures are considered (from left to right $\beta = 1, 2, 3, 4, 5$ and 6) as well as dimensions: $d = 2$ (dashed curves) and mean-field $d = \infty$ (full curves).

B. Out-of-equilibrium dynamics

We now consider the out-of-equilibrium behaviour of the models, in particular the decay of the concentration of particles (energy density) $c(t) \equiv N^{-1}\langle H(t) \rangle$, after a quench from an infinite temperature to a low temperature T at time $t = 0$. This decay shows an interesting structure with two intermediate plateaux when the diffusive constant D and the final temperature T are such that $e^{-2\beta} \ll D \ll 1$. The first regime is dominated by the annihilation process

and leads to a configuration with less than three particles on the same site. This first regime occurs on a timescale of order 1. Then, the diffusion process comes into play on a timescale of order D^{-1} and the dimers diffuse until they reach a single particle and annihilate. Then the system reaches a configuration with mainly isolated particles. Finally, in order to reach the equilibrium concentration of particles, the activated regime involving the effective motion of isolated particles through the creation or annihilation of dimers is necessary and occurs on a timescale of order $e^{2\beta}$.

The last regime in the concentration decay (before the equilibrium concentration is reached) may also be seen as either $A + A \rightarrow \emptyset$ or $A + B \rightarrow \emptyset$ reaction-diffusion processes, depending on the models, since the particles have to pair themselves in order to disappear. Those two processes have different critical behaviours and critical dimensions: $d_c = 2$ for the former and $d_c = 4$ for the later. As a consequence, we expect a power law decay:

$$c(t) \sim (e^{2\beta}/t)^\alpha \quad (23)$$

with $\alpha = 1$ above the critical dimension d_c , while below the critical dimension $d < d_c$, $\alpha = d/2$ for the $A + A \rightarrow \emptyset$ case, and $d/4$ for the $A + B \rightarrow \emptyset$ case [14,15] (at the critical dimension there may be logarithmic corrections).

In Fig. 4 (left) we present numerical simulations for different dimensions and a diffusive constant $D = 10^{-4}$ of the concentration decay for the model with a single type of particles. The temperature after the quench is $T = 1/10$, so the different timescales are well separated ($1 \ll D^{-1} \ll e^{2\beta}$), and the decay presents a two plateau structure. The first plateau is roughly independent of the dimension whereas the second plateau decreases with increasing dimensions to reach the mean-field value. Notice that the qualitative behaviour is maintained even in the mean-field limit. The dynamics during the last stage of the decay corresponds to a power law decay with the expected critical exponents α . Fig. 4 (right) shows similar results for the model with two types of particles, but with a diffusive constant $D = 1$. The diffusive timescale is now equivalent to the annihilation one, and the decay presents a single plateau structure. Again, we see the critical behaviour during the last stage of the decay, with the critical exponents α expected from the theory.

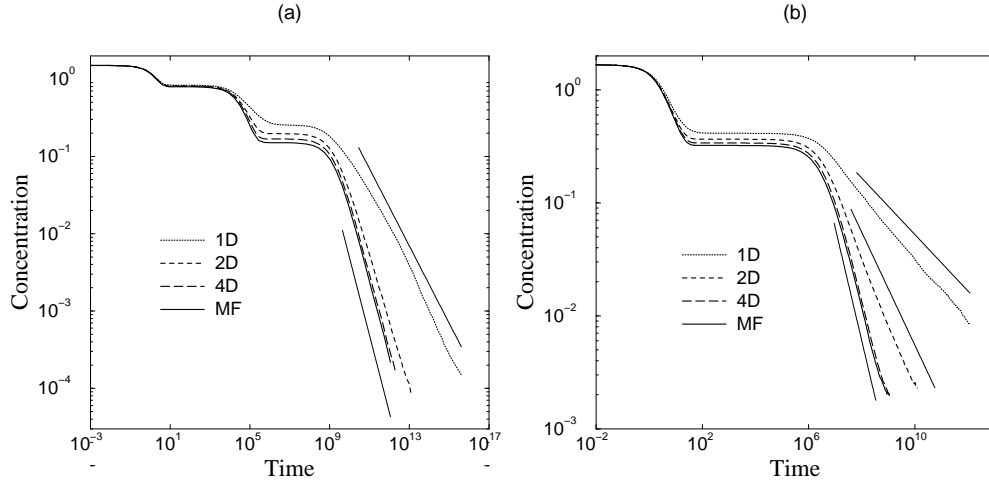


FIG. 4. (Left) Concentration of particles for the model with a single type of particles after a quench from $T = \infty$ to $T = 1/10$ with a diffusive constant $D = 10^{-4}$ and for different dimensions ($d = 1, 2$ and 4 and mean-field). The $A + A \rightarrow \emptyset$ reaction-diffusion process during the second decay is illustrated by the change in power law for $d < d_c = 2$. The two straight lines correspond to the expected exponents $\alpha = 1$ and $\alpha = 1/2$. (Right) Model with two different types of particles, and diffusive constant $D = 1$. The straight lines correspond to the expected power law decays corresponding to $A + B \rightarrow \emptyset$ reaction-diffusion processes in different dimensions: for $d < d_c = 4$, $\alpha = d/4$, while $\alpha = 1$ for $d \geq d_c$.

In what follows we will concentrate mainly on the model with one kind of particle.

IV. MEAN-FIELD SOLUTION

The mean-field version of the model where all sites are neighbors allows to write exact evolution equations for the probability $p_n^i(t)$ of a site i to be occupied by n particles at time t . The dynamical equations for $p_n^i(t)$ read:

$$\frac{dp_0^i}{dt} = -p_0^i p_3 + p_3^i (1 - p_3) - D p_0^i (p_2 + p_3) + D p_2^i (p_0 + p_1) - e^{-2\beta} p_0^i (1 - p_0) + e^{-2\beta} p_1^i p_0, \quad (24a)$$

$$\frac{dp_1^i}{dt} = -p_1^i p_3 + p_0^i p_3 - D p_1^i (p_2 + p_3) + D p_3^i (p_0 + p_1) - e^{-2\beta} p_1^i p_0 + e^{-2\beta} p_2^i p_0, \quad (24b)$$

$$\frac{dp_2^i}{dt} = -p_2^i p_3 + p_1^i p_3 - D p_2^i (p_0 + p_1) + D p_0^i (p_2 + p_3) - e^{-2\beta} p_2^i p_0 + e^{-2\beta} p_3^i p_0, \quad (24c)$$

$$\frac{dp_3^i}{dt} = -p_3^i (1 - p_3) + p_2^i p_3 - D p_3^i (p_0 + p_1) + D p_1^i (p_2 + p_3) - e^{-2\beta} p_3^i p_0 + e^{-2\beta} p_0^i (1 - p_0). \quad (24d)$$

The time dependence has been omitted for conciseness and the sum over the neighbors has been performed using the fact that the probabilities p_n^j are indeed independent of the site j :

$$\frac{1}{N-1} \sum_{j \neq i} p_n^j = p_n = p_n^i. \quad (25)$$

Notice that the right hand side of each of the equations (24) comprises three pairs of terms, each pair corresponding to a particular process, annihilation, diffusion and creation, with their respective rates.

The dynamical equations satisfy the conservation of probability, $\sum_n p_n^i = 1$, which reduces the number of independent variables to only three, for example p_0, p_1 and p_2 , in the mean-field model. The trivial equilibrium probabilities:

$$p_n^{eq} = e^{-\beta n} \left(\sum_{k=0}^3 e^{-\beta k} \right)^{-1} \quad (26)$$

are a stationary solution of Eqs. (24). Equations (24) can be solved numerically to arbitrary accuracy. However, it is also helpful to consider their approximate solution, regime by regime, to better illustrate the underlying physics.

A. Concentration decay after a quench

After a quench from infinite temperature to a temperature $T = 1/\beta$, the energy per site or concentration of particles $c(t)$ decays from $c(0) = 3/2$ [$p_n(0) = 1/4$ for all $n \leq 3$] to its equilibrium value

$$c(\infty) = c_{eq}(\beta) = \left(\sum_{k=0}^3 k e^{-\beta k} \right) \left(\sum_{k=0}^3 e^{-\beta k} \right)^{-1}. \quad (27)$$

If T is low and the diffusive constant small, such that $e^{-2\beta} \ll D \ll 1$, the energy decay may be decomposed into three different regimes. The first regime corresponds to the disappearance of sites with 3 particles due to the annihilation process and leads to a first plateau in the decay. The diffusion comes into play in the second regime and leads to a second plateau. On this plateau the particles are essentially isolated. The last regime is an activated one where the creation process is necessary to reach the equilibrium concentration. In previous models [11–13], where the diffusive timescale of dimers was equivalent to their annihilation timescale, the first plateau discussed here was absent.

1. First regime: zero temperature and no diffusion

In the first regime, we assume that only the annihilation process can occur. The equations (24) simplify, and only the two first terms on the right hand side are relevant. The probability p_3 decays to $p_3 = 0$, and, assuming that p_2 stays constant, we get a good approximation for the different probabilities $p_n(t)$ (See appendix A and Fig. 5). The probabilities p_n corresponding to the first plateau of the concentration decay are given by:

$$\tilde{p}_0 \simeq 0.458, \quad \tilde{p}_1 \simeq 0.287, \quad \tilde{p}_2 \simeq 1/4, \quad \tilde{p}_3 \simeq 0. \quad (28)$$

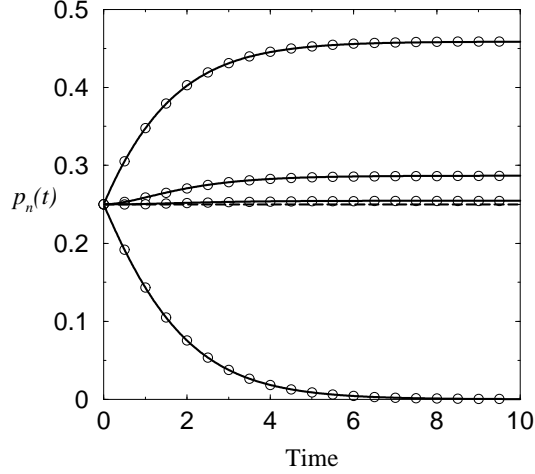


FIG. 5. Probabilities $p_n(t)$ during the first regime of the energy decay. From top to bottom: p_0, p_1, p_2 and p_3 . Symbols correspond to simulations and lines to the numerical solution of the exact equations (full lines) and the analytical approximation (dashed lines). The difference between the two sets of lines is only visible for p_2 .

2. Second regime: zero temperature and slow diffusion

For slow diffusion, $D \ll 1$, the first regime occurs on a timescale $t \sim O(1)$. For times $t \sim O(D^{-1})$ diffusion comes into play. The probability p_3 for a site to be occupied by 3 particles saturates to a quantity of order D . From (24d), noticing that $dp_3/dt \sim O(D^2)$ and thus negligible,

$$p_3 \simeq D \frac{p_1 p_2}{p_0 + p_1}. \quad (29)$$

From the final probabilities \tilde{p}_n from the first regime, given by Eq.(28), it is possible to determine the value of the second plateau in the concentration decay. Replacing the expression (29) for p_3 in Eqs. (24b) and (24c), we obtain:

$$\frac{dp_1}{dp_2} = \frac{2p_1}{1 - p_1} \quad (30)$$

which can be integrated from $\tilde{p}_2 = 1/4$ to $p_2(t)$ [with $t \sim O(D^{-1})$]. This leads to

$$\ln p_1(t) - p_1(t) - \ln \tilde{p}_1 + \tilde{p}_1 = 2p_2(t) - 2\tilde{p}_2. \quad (31)$$

Knowing that the particles are essentially isolated during this second plateau, the probabilities $p_n(\infty) = \bar{p}_n$ are then:

$$\bar{p}_0 \simeq 0.85, \quad \bar{p}_1 \simeq 0.15, \quad \bar{p}_2 \simeq 0, \quad \bar{p}_3 \simeq 0. \quad (32)$$

3. Third regime: activation and slow diffusion

The third regime corresponds to the activated regime where the system has to overcome an energy barrier to reach equilibrium, and occurs on a timescale $t \sim e^{2\beta}$. An analogy in this third regime may be drawn with a reaction-diffusion process of the type $A + A \rightarrow \emptyset$. When two isolated particles moving with an effective diffusive constant $e^{-2\beta}$ through successive creation-annihilation processes pair up, this pair diffuse on a faster timescale ($\sim D^{-1}$) before they disappear when it reaches another isolated particle. We therefore expect a power law decay of the concentration during the last regime.

In order to confirm this observation we first need to determine the probabilities p_2 and p_3 up to the order $e^{-2\beta}$, neglecting dp_2/dt and dp_3/dt which are of order $e^{-4\beta}$. From (24c) and (24d) we deduce:

$$p_3 \simeq e^{-2\beta} p_1, \quad Dp_2 \simeq e^{-2\beta} (Dp_0 + p_1). \quad (33)$$

Replacing these expressions in (24b),

$$\frac{dp_1}{dt} \simeq -2e^{-2\beta} p_1^2 \quad (34)$$

we obtain the mean-field equation for the reaction-diffusion process $A + A \rightarrow \emptyset$ with an effective diffusion constant $e^{-2\beta}$. The solution of this equation is:

$$p_1(t) \simeq \frac{\bar{p}_1}{1 + 2e^{-2\beta}\bar{p}_1(t - \bar{t})} \quad (35)$$

with \bar{t} an initial time onto the second plateau of the concentration decay ($D^{-1} \ll \bar{t} \ll e^{2\beta}$). $\bar{t} \simeq 50D^{-1}$ is a good estimate for $D = 10^{-3}$ and $T = 1/10$ (see Fig. 6).

From Eq. (35) it seems that the concentration does not reach its equilibrium value $c_{eq} \sim e^{-\beta}$ but decays to zero asymptotically. In order to account for the approach to equilibrium we need to include in (34) terms of order $e^{-4\beta}$ previously neglected, which become relevant when $p_1 \sim e^{-\beta}$. Taking into account leading order terms in $e^{-4\beta}$ (which means neglecting terms of order $p_1 e^{-4\beta}$, which are always negligible), we obtain:

$$\frac{dp_1}{dt} = -2e^{-2\beta} (p_1^2 - e^{-2\beta}) \quad (36)$$

which has for solution:

$$p_1(t) = e^{-\beta} \frac{\bar{p}_1 + e^{-\beta} + (\bar{p}_1 - e^{-\beta}) e^{-4e^{-3\beta}(t - \bar{t})}}{\bar{p}_1 + e^{-\beta} - (\bar{p}_1 - e^{-\beta}) e^{-4e^{-3\beta}(t - \bar{t})}}. \quad (37)$$

For a timescale $t \sim O(e^{2\beta})$ we recover the behaviour (35) but for a timescale $t \sim O(e^{3\beta})$ the concentration reaches the equilibrium one as:

$$c(t) \simeq p_1(t) \simeq e^{-\beta} \left(1 + 2e^{-4e^{-3\beta}(t - \bar{t})} \right) \quad (38)$$

leading to an equilibration time $\tau_{eq} \simeq e^{3\beta}$ larger than the relaxation time $\tau \simeq e^{2\beta}$ deduced from equilibrium autocorrelation.

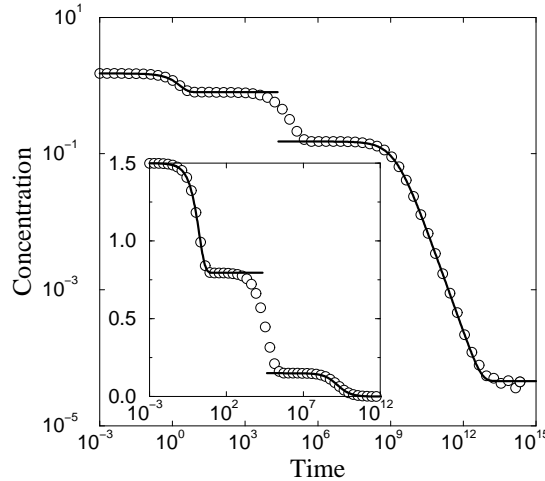


FIG. 6. Concentration decay as function of time after a quench to the temperature $T = 1/10$ and for a diffusive constant $D = 10^{-4}$. Symbols correspond to numerical simulations, and lines to the analytical results for the first and third regimes. Inset: $T = 1/6$.

B. Out-of-equilibrium correlation and response

We now concentrate on the behaviour of two-time quantities, like correlation and response functions, in the out-of-equilibrium regime.

1. Correlation functions

From the two-time out-of-equilibrium autocorrelation functions

$$C_{n,n'}(t, t_w) = \langle \delta_{n_i(t), n} \delta_{n_i(t_w), n'} \rangle \quad (39)$$

with initial conditions

$$C_{n,n'}(t_w, t_w) = p_n(t_w) \delta_{n,n'} \quad (40)$$

it is possible to construct all relevant two point autocorrelations, and in particular

$$C(t, t_w) \equiv \langle n_i(t) n_i(t_w) \rangle = \sum_{n,n'} n n' C_{n,n'}(t, t_w). \quad (41)$$

The correlation functions $C_{n,n'}$ correspond to the probabilities of having n particles at time t on a given site when there were n' particles at time $t_w \leq t$ on this particular site. They satisfy the equations (24) replacing $p_n^i(t)$ by $C_{n,n'}(t, t_w)$ but keeping the probabilities $p_n(t)$. This leads to an explicitly time dependent linear system of equations for the autocorrelations.

In the following we concentrate on waiting times $t_w \gg D^{-1}$, that is, after the second plateau in the concentration decay. In this case, sites have mainly at most one particle. The probabilities to have 2 or 3 particles on a given site are small and satisfy the equations (33). The only relevant correlation function among $C_{n,n'}$ is $C_{1,1}$, and $C(t, t_w) \simeq C_{1,1}(t, t_w)$. The correlation functions with n or n' larger than one are at least of order $e^{-2\beta}$ smaller, whereas those with $n = 0$ or $n' = 0$ do not affect $C(t, t_w)$. A simple calculation (see appendix B) leads the following differential equation for $C_{1,1}$

$$\frac{dC_{1,1}}{dt}(t, t_w) = -C_{1,1}(t, t_w) \left[1 + 2p_1(t) + \frac{D}{1+D} \right] e^{-2\beta} + \left(1 + \frac{D}{1+D} \right) p_1(t_w) p_1(t) e^{-2\beta}. \quad (42)$$

with the solution

$$C_{1,1}(t, t_w) = p_1(t) \left[p_1(t_w) + (1 - p_1(t_w)) e^{-(t-t_w)/\tau_c} \right]. \quad (43)$$

The correlation time τ_c is given by:

$$\tau_c = e^{2\beta} \left(1 + \frac{D}{1+D} \right)^{-1}. \quad (44)$$

From this solution we recover that $C_{1,1}(t, t) = p_1(t)$, which is given by (37).

Fig. 7 presents the autocorrelations $C_{1,1}(t, t)$ and $C_{1,1}(t, t_w)$ for two different waiting times $t_w = 10^4$ and 10^6 as function of the time difference $t - t_w$. The temperature is $T = 1/6$ and the diffusive constant $D = 10^{-2}$. The analytical results Eqs.(37) and (43) agree with the numerical simulations for a system size $N = 10^6$.

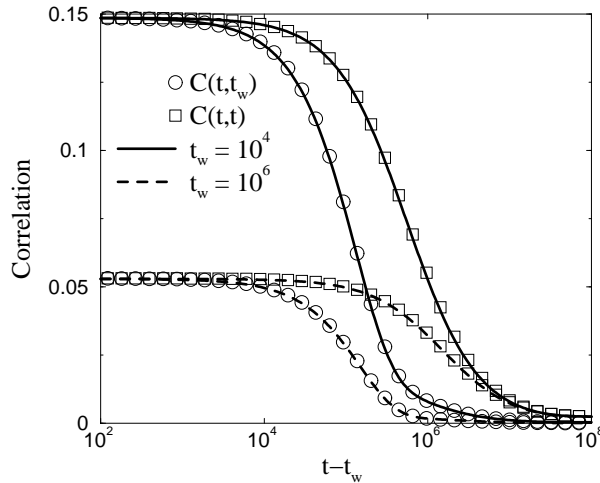


FIG. 7. Out-of-equilibrium $C_{1,1}(t, t_w)$ (circles) and $C_{1,1}(t, t)$ (squares) after a quench to temperature $T = 1/6$. Symbols correspond to simulations and lines to the analytical result. Waiting times are $t_w = 10^4$ (full lines) and 10^6 (dashed lines), and the diffusion constant $D = 10^{-2}$.

2. Response functions

In order to determine the out-of-equilibrium response function, we need to introduce a perturbation at time t_w after the quench. Different perturbations are possible but to get a response related to the autocorrelation, it is common to consider a random field on each site coupled to the corresponding observable [24]. The simplest possibility is to couple the random field to the single occupancy operator $\delta_{n_i,1}$, leading to the perturbation

$$\delta H = -h \sum_i \epsilon_i \delta_{n_i,1}. \quad (45)$$

h is the strength of the field and will have to be small enough to stay in the linear regime. The random variables ϵ_i may be Gaussian variables or Ising spins ($\epsilon_i = \pm 1$) with zero mean and unit variance. The corresponding (integrated) response function is the change in the expectation value of $\delta_{n(t),1}$ due to the perturbation,

$$\chi_1(t, t_w) = \overline{h^{-1} N^{-1} \sum_i \epsilon_i \langle \delta_{n_i(t),1} \rangle_h} \quad (46)$$

where the overline stands for the average over the random field variables. This response is conjugate to the autocorrelation $C_{1,1}(t, t')$, which as was shown above is the relevant one for long times and low temperatures,

$$\overline{N^{-1} \sum_{i,j} \epsilon_i \epsilon_j \langle \delta_{n_i(t),1} \delta_{n_j(t'),1} \rangle} = C_{1,1}(t, t'). \quad (47)$$

The definition of the perturbation is not enough to determine the response. We also have to define how this perturbation affects the dynamical rules, maintaining the detailed balance conditions in order to ensure equilibrium asymptotically. Once again different definitions are possible. We will consider two of them. The natural definition of the perturbed dynamics is to use for the rates a Metropolis rule with the perturbed Hamiltonian $H + \delta H$,

$$\min(1, e^{-\beta \Delta(H + \delta H)}) \quad (\text{M}) \quad (48)$$

where $\Delta(H + \delta H)$ corresponds to the change in the perturbed Hamiltonian under the corresponding transition. One disadvantage is that this definition will only extract a response from unoccupied sites. A second possibility is to modify the dynamical rules by multiplying the unperturbed rates by another Metropolis factor

$$\min(1, e^{-\beta \Delta(\delta H)}) \times \min(1, e^{-\beta \Delta(H)}) \quad (\text{MM}) \quad (49)$$

It is easy to see that this modification of the dynamical rules preserves detailed balance with respect to $H + \delta H$. The advantage is that this definition allows to extract a response from occupied and unoccupied sites. For simple spin facilitated models the two dynamics yield equivalent responses, the second one being more efficient from the numerical point of view. We will see below that this equivalence does not hold for the present models.

In order to determine the response function analytically we assume that only the site i is perturbed. Its probabilities $p_n^i(t)$ are modified accordingly:

$$p_n^i(t) = p_n(t) + h \epsilon_i \chi_n(t, t_w) \quad (50)$$

where $p_n(t)$ are the unperturbed probabilities. The equations (24) have to be modified to take into account the change of rates. The zeroth order in h gives back the dynamical equations (24) for the unperturbed $p_n(t)$. The first order in h leads to a system of equations for the responses $\chi_n(t, t_w)$ (see appendix C).

For the perturbation (45), the only relevant response function is $\chi_1(t, t_w)$. For the case of the modified Metropolis (MM) it satisfies (see details of the calculation in appendix C)

$$\frac{d}{dt} \chi_1^{(\text{MM})}(t, t_w) = - \left(1 + 2p_1(t) + \frac{D}{1+D} \right) \chi_1^{(\text{MM})}(t, t_w) e^{-2\beta} + \beta p_1(t) \left(1 + \frac{D}{1+D} - \frac{D p_1(t)}{2(1+D)} \right) e^{-2\beta}. \quad (51)$$

Neglecting the third term in the last parenthesis leads to the following approximation:

$$\chi_1^{(\text{MM})}(t, t_w) = \beta p_1(t) \left(1 - e^{-(t-t_w)/\tau_c} \right) \quad (52)$$

with the time τ_c already defined for the correlation function, Eq. (44). The timescale involved in the response and correlation function is thus identical. Fig. 8 shows the accuracy of this analytic result. The response function is non-monotonic, a common feature of the activated regime [9,25], and also observed in models of vibrated granular matter [28,29]. In the present case the non-monotonic behaviour is given by the fact that the response is the product of a decreasing function, $p_1(t)$, corresponding to the number of defects able to respond, and an increasing one, $1 - e^{-(t-t_w)/\tau_c}$, corresponding to the monotonic rescaled equilibrium response function. The scaling from of the response function given in (52) is analogous to that in the Fredrickson–Andersen model [25]. The corresponding calculation for the case of the Metropolis (M) dynamics gives

$$\chi_1^{(M)}(t, t_w) = \chi_1^{(MM)}(t, t_w) - 2\beta\Delta(t, t_w) \quad (53)$$

where

$$\Delta(t, t_w) \equiv p_1(t) \left[p_1(t) - p_1(t_w) e^{-(t-t_w)/\tau_c} \right] \quad (54)$$

The two responses (52) and (53) are different. Given that the second term inside the brackets in (54) decays faster than the first one [see Eqs. (35,37,38)], $\Delta(t, t_w)$ is always positive, and $\chi_1^{(M)} \leq \chi_1^{(MM)}$, as expected.

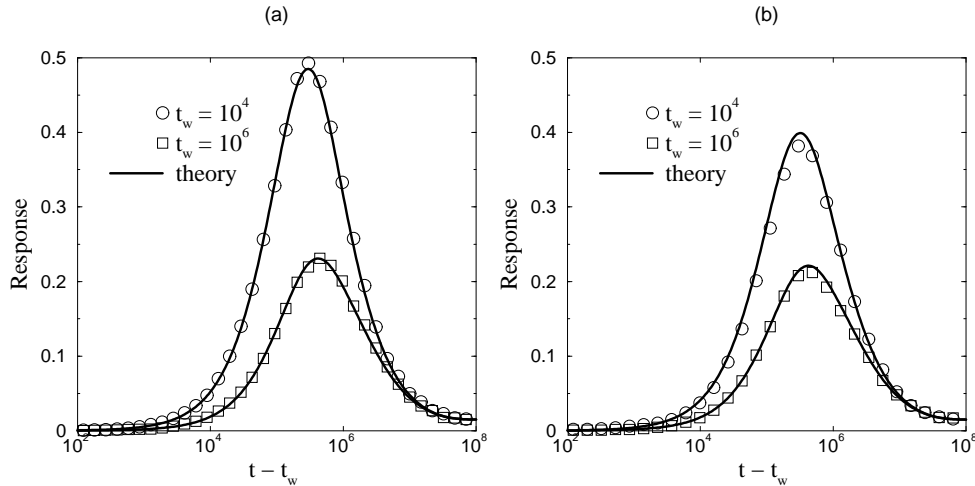


FIG. 8. Out-of-equilibrium response $\chi_1(t, t_w)$ for (a) MM dynamics, and (b) M dynamics, as a function of $t - t_w$, at temperature $T = 1/6$, for waiting times $t_w = 10^4$ (circles) and 10^6 (squares), and a diffusive constant $D = 10^{-2}$. The lines correspond to the analytical result.

3. Fluctuation–dissipation relations

Having obtained correlation and response functions, we can now study out-of-equilibrium fluctuation–dissipation (FD) relations [26]. Since we are considering the case of long but finite times, and therefore one-time quantities are still changing with time, FD relations have to be considered between the integrated response, $\chi_1(t, t_w)$, and the difference of the conjugate connected correlation functions, $C_{1,1}^{(c)}(t, t) - C_{1,1}^{(c)}(t, t_w)$, where $C_{1,1}^{(c)}(t, t') \equiv C_{1,1}^{(c)}(t, t') - p_1(t)p_1(t')$ (see [25] for a discussion). In Figs. 9(a) and 9(b) we show the FD plots for the case of MM and M dynamics, respectively, for temperature $T = 1/6$ and waiting times $t_w = 10^4$ and 10^6 (inset).

There are several things to note. First, despite the fact that both response functions and difference of connected correlations are non-monotonic in t (which implies that the FD curves when plotted parametrically for fixed t_w start from the origin, go up, and then come back again), to a very good approximation $\chi_1(t, t_w) = \chi_1[C_{1,1}^{(c)}(t, t) - C_{1,1}^{(c)}(t, t_w)]$, similarly to what was found for other simple strong glass formers [25]. Second, the FD curves approach the fluctuation–dissipation theorem (FDT) value as waiting time is increased, as expected. Third, the FD relations look almost linear (although this may be just a consequence of the fact that the departure from FDT is relatively small). In this case the FDT violation ratio $X(t, t_w)$ [27,26] is just a function of the waiting time, $X = X(t_w)$.

We see from Figs. 9(a) and 9(b) that $X > 1$ for the case of MM dynamics, while $X < 1$ for the case of M dynamics. This can be traced back to Eqs. (43,52,53), which lead to $T\chi_1(t, t_w) = C_{1,1}^{(c)}(t, t) - C_{1,1}^{(c)}(t, t_w) \pm \Delta(t, t_w)$, where the

upper (lower) sign corresponds to MM (M) dynamics, together with the fact that $\Delta(t, t_w) \geq 0$ for all times. An approximation to the value of $X(t_w)$ can be obtained from the following argument. The slope with which the FD curves leave the origin corresponds to the time regime in which the exponential in the second term of Eq. (54) decreases much more rapidly than $p_1(t)$ [see Eq. (35)]. If we assume that $p_1(t)$ does not change at all in this initial period, we may approximate $\Delta(t, t_w) \sim p_1^2(t_w) (1 - e^{-(t-t_w)/\tau_c})$. This in turn gives for the FD ratio $X(t_w) \sim [1 \mp p_1(t_w)]^{-1}$, with the upper (lower) sign corresponding to MM (M) dynamics. For the plots of Fig. 9(a) this approximation predicts $X(t_w) \sim 1.18, 1.05$ for $t_w = 10^4, 10^6$, while a linear fit to the data gives $X_{\text{fit}}(t_w) = 1.11, 1.04$ [$X(t_w) \sim 0.85, 0.95$ and $X_{\text{fit}}(t_w) = 0.89, 0.96$ for Fig. 9(b), respectively].

Finally, in Fig.9(c) we compare the behaviour in the mean-field model with that at finite dimensions. For $d = 1$ FDT is obeyed, similar to what happens in the Fredrickson–Andersen model [25]. For $d \geq d_c = 2$ however, the FD plots coincide with the mean-field ones. This indicates that the aging behaviour is controlled by the out-of-equilibrium critical point of the underlying diffusion–annihilation process, and that mean-field serves as a good approximation for the physically relevant dimensions $d = 2, 3$.

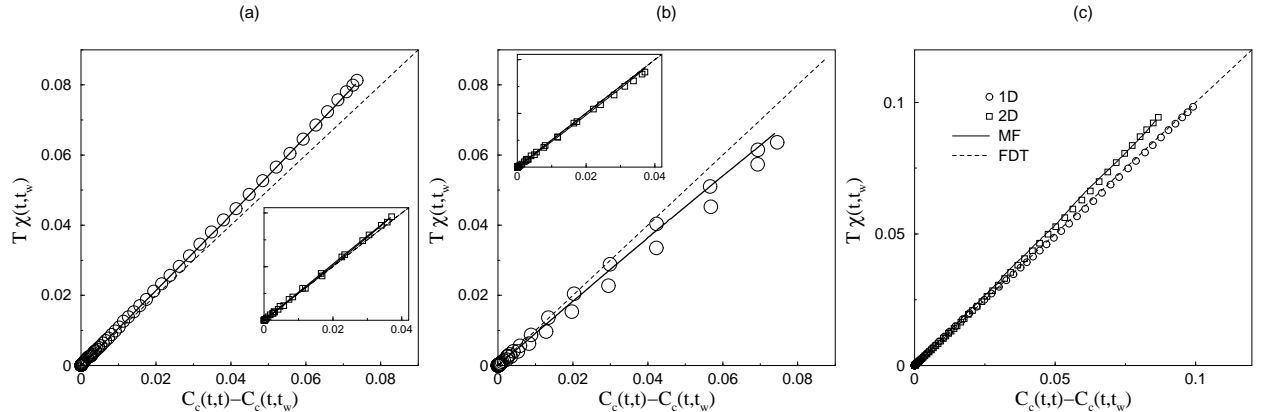


FIG. 9. (a) FD plot for MM dynamics at $T = 1/6$ and waiting time $t_w = 10^4$ (inset: $t_w = 10^6$). The symbols correspond to simulations, the full lines to the analytical result, and the dashed line to FDT. (b) Similar plot for M dynamics. (c) FD plots in various dimensions (for MM dynamics): $d = 1$ (circles), $d = 2$ (squares), and MF (full line); $T = 1/6$, $t_w = 10^4$.

V. CONCLUSIONS

In this paper we have introduced simple models inspired by covalent glasses and topological froths. The models display strong glass forming behaviour despite their trivial thermodynamic properties due to the presence of constraints to the dynamics which generate dynamical frustration. We have studied the connection with underlying diffusion–annihilation processes, and have shown that the aging dynamics of these models is dominated by the critical out-of-equilibrium fixed point of the associated diffusion–annihilation theory. We formulated a mean-field version of the models, which keeps most of the features of the finite dimensional ones, and which allows for an extremely accurate analytical solution of the low temperature out-of-equilibrium aging dynamics in the low temperature regime where activated processes play a dominant role.

ACKNOWLEDGMENTS

This work was supported by EU Grant No. HPMF-CT-1999-00328, the Glasstone Fund, and EPSRC Programme Grant GR/R83712.

APPENDIX A: FIRST REGIME IN THE CONCENTRATION DECAY

The first regime in the concentration decay may be obtained by considering the dynamics at zero temperature and without diffusion ($D = 0$). The dynamical equations reduce to:

$$\frac{dp_0}{dt} = p_3(p_1 + p_2) \quad (\text{A1})$$

$$\frac{dp_1}{dt} = p_3(p_0 - p_1) \quad (\text{A2})$$

$$\frac{dp_2}{dt} = p_3(p_1 - p_2) \quad (\text{A3})$$

$$\frac{dp_3}{dt} = -p_3(p_0 + p_1) \quad (\text{A4})$$

with the infinite temperature probabilities $p_n = 1/4$ as initial conditions. Notice that the right hand side of the equations is proportional to p_3 and the derivative of p_3 is negative indicating that a first plateau will be reached when $p_3 = 0$ with non-zero values for the probabilities p_0, p_1 and p_2 .

In the absence of diffusion, p_2 remains approximately constant at its initial value, $p_2(t) \simeq 1/4$. Notice that if the initial configuration (before the quench) does not correspond to one at infinite temperature, this approximation is no longer valid. Using $p_0 + p_1 = 1 - p_2 - p_3 = 3/4 - p_3$ and (A4), we are able to deduce:

$$p_3(t) = \frac{3e^{-3t/4}}{2 + e^{-3t/4}}. \quad (\text{A5})$$

The probabilities p_0 and p_1 are determined considering the linear combinations $a_{\pm}p_0 + p_1$ with $a_{\pm} = \frac{1}{2}(1 \pm \sqrt{5})$ which satisfy the following differential equation:

$$\frac{d}{dt}(a_{\pm}p_0 + p_1) = \frac{p_3}{a_{\pm}}(a_{\pm}p_0 + p_1 + a_{\pm}^2/4). \quad (\text{A6})$$

A solution is given by:

$$\frac{4(a_{\pm}p_0(t) + p_1(t) + a_{\pm}^2/4)}{a_{\pm} + 1 + a_{\pm}^2} = \left(\frac{3}{2 + e^{-3t/4}}\right)^{1/a_{\pm}}. \quad (\text{A7})$$

We deduce the following approximations:

$$p_0(t) = -\frac{1}{4} + \frac{3 + \sqrt{5}}{4\sqrt{5}}A^{\frac{\sqrt{5}-1}{2}} - \frac{3 - \sqrt{5}}{4\sqrt{5}}A^{-\frac{\sqrt{5}+1}{2}} \quad (\text{A8})$$

$$p_1(t) = -\frac{1}{4} + \frac{1 + \sqrt{5}}{4\sqrt{5}}A^{\frac{\sqrt{5}-1}{2}} + \frac{\sqrt{5}-1}{4\sqrt{5}}A^{-\frac{\sqrt{5}+1}{2}} \quad (\text{A9})$$

with $A = 3/(2 + e^{-3t/4})$.

APPENDIX B: OUT-OF-EQUILIBRIUM CORRELATION FUNCTION

Here we determine the out-of-equilibrium correlations $C_{n,n'}$. They satisfy the equations (24), with the replacement of p_n^i by $C_{n,n'}$. Since all correlations with $n \geq 2$ or $n' \geq 2$ are at least of order $e^{-2\beta}$, and the ones with $n = 0$ or $n' = 0$ are irrelevant for the correlation $C(t, t_w)$, we concentrate on the set of equations corresponding to $n' = 1$:

$$\frac{dC_{0,1}}{dt} = -C_{0,1}p_3 + C_{3,1}(1 - p_3) - DC_{0,1}(p_2 + p_3) + DC_{2,1}(p_0 + p_1) - e^{-2\beta}C_{0,1}(1 - p_0) + e^{-2\beta}C_{1,1}p_0, \quad (\text{B1})$$

$$\frac{dC_{1,1}}{dt} = -C_{1,1}p_3 + C_{0,1}p_3 - DC_{1,1}(p_2 + p_3) + DC_{3,1}(p_0 + p_1) - e^{-2\beta}C_{1,1}p_0 + e^{-2\beta}C_{2,1}p_0, \quad (\text{B2})$$

$$\frac{dC_{2,1}}{dt} = -C_{2,1}p_3 + C_{1,1}p_3 - DC_{2,1}(p_0 + p_1) + DC_{0,1}(p_2 + p_3) - e^{-2\beta}C_{2,1}p_0 + e^{-2\beta}C_{3,1}p_0, \quad (\text{B3})$$

$$\frac{dC_{3,1}}{dt} = -C_{3,1}(1 - p_3) + C_{2,1}p_3 - DC_{3,1}(p_0 + p_1) + DC_{1,1}(p_2 + p_3) - e^{-2\beta}C_{3,1}p_0 + e^{-2\beta}C_{0,1}(1 - p_0). \quad (\text{B4})$$

Equations (B3) and (B4) allow to obtain $C_{2,1}$ and $C_{3,1}$ as functions of $C_{1,1}$ and $C_{0,1}$, neglecting their derivatives and using (33),

$$\begin{aligned} DC_{2,1} &= e^{-2\beta} (C_{0,1}(p_1 + D) + C_{1,1}p_1), \\ (1 + D)C_{3,1} &= e^{-2\beta} (C_{1,1}(p_1 + D) + C_{0,1}p_1). \end{aligned} \quad (\text{B5})$$

$$(\text{B6})$$

Combining all these results and the fact that $C_{0,1}(t, t_w) + C_{1,1}(t, t_w) \simeq p_1(t_w)$, we deduce an equation for $C_{1,1}$:

$$\frac{dC_{1,1}}{dt}(t, t_w) = -C_{1,1}(t, t_w) \left(1 + 2p_1(t) + \frac{D}{1+D} \right) e^{-2\beta} + \left(1 + \frac{D}{1+D} \right) p_1(t)p_1(t_w)e^{-2\beta}. \quad (\text{B7})$$

$\mathcal{C}(t, t_w) = p_1(t)p_1(t_w)$ is a trivial solution of this equation. A general solution is then $C_{1,1}(t, t_w) = \mathcal{C}(t, t_w) + \tilde{C}(t, t_w)$ with:

$$\frac{d\tilde{C}}{dt}(t, t_w) = -\tilde{C}(t, t_w) \left(1 + 2p_1(t) + \frac{D}{1+D} \right) e^{-2\beta}. \quad (\text{B8})$$

The solution of this linear differential equation is:

$$\tilde{C}(t, t_w) = \tilde{C} \exp \left(-\frac{t-t_w}{\tau_c} - \int_{t_w}^t 2e^{-2\beta} p_1(t') dt' \right). \quad (\text{B9})$$

with $\tau_c = (1 + D/(1 + D))^{-1} e^{2\beta}$. Using (34), we deduce:

$$\tilde{C}(t, t_w) = \hat{C} \frac{p_1(t)}{p_1(t_w)} \exp \left(-\frac{t-t_w}{\tau_c} \right). \quad (\text{B10})$$

The parameter \hat{C} is obtained from the initial condition $C_{1,1}(t_w, t_w) = p_1(t_w)$ leading to the correlation:

$$C_{1,1}(t, t_w) = p_1(t) \left(p_1(t_w) + (1 - p_1(t_w))e^{-(t-t_w)/\tau_c} \right). \quad (\text{B11})$$

APPENDIX C: OUT-OF-EQUILIBRIUM RESPONSE FUNCTION

In this appendix we determine the out-of-equilibrium response function corresponding to a perturbation (45) in the case of MM dynamics (49). This prescription leads to a different response for spins with $\epsilon = 1$ and -1 . The response is determined assuming only spin i is perturbed at a time t_w after the quench at $t = 0$. The corresponding probability of occupancies are slightly modified compared to the unperturbed case:

$$p_n^i(t) = p_n(t) + h\epsilon_i \chi_n^{\epsilon_i}(t, t_w) \quad (\text{C1})$$

which defines the two sets of response functions $\chi_n^{\epsilon_i}(t, t_w)$ for a perturbed spin with different random variable $\epsilon_i = \pm 1$. The total response for a given n is simply the average between the two responses for different ϵ_i . The response functions are determined from the first order expansion in powers of the field h of the modified equations (24). χ_2 and χ_3 have a higher order in $e^{-2\beta}$ than χ_0 and χ_1 . From the conservation of the probability, it follows that $\chi_0 = -\chi_1$ and we may take χ_1 as the only relevant response function. In order to determine χ_1 we need the equations for p_1^i and p_3^i for a random variable $\epsilon_i = 1$

$$\frac{dp_1^i}{dt} = -e^{-\beta h} p_1^i p_3 + p_0^i p_3 - D e^{-\beta h} p_1^i (p_2 + p_3) + D p_3^i (p_0 + p_1) - e^{-2\beta - \beta h} p_1^i p_0 + e^{-2\beta} p_2^i p_0, \quad (\text{C2})$$

$$\frac{dp_3^i}{dt} = -p_3^i (1 - p_3) + p_2^i p_3 - D p_3^i (p_0 + p_1) + D e^{-\beta h} p_1^i (p_2 + p_3) - e^{-2\beta} p_3^i p_0 + e^{-2\beta} p_0^i (1 - p_0), \quad (\text{C3})$$

while for $\epsilon_i = -1$:

$$\frac{dp_1^i}{dt} = -p_1^i p_3 + e^{-\beta h} p_0^i p_3 - D p_1^i (p_2 + p_3) + D e^{-\beta h} p_3^i (p_0 + p_1) - e^{-2\beta} p_1^i p_0 + e^{-2\beta - \beta h} p_2^i p_0, \quad (\text{C4})$$

$$\frac{dp_3^i}{dt} = -p_3^i (1 - p_3) + p_2^i p_3 - D e^{-\beta h} p_3^i (p_0 + p_1) + D p_1^i (p_2 + p_3) - e^{-2\beta} p_3^i p_0 + e^{-2\beta} p_0^i (1 - p_0). \quad (\text{C5})$$

Using (33) and neglecting the time derivative of $\chi_3^{\epsilon_i}$, the resulting equations for $\chi_n^{\epsilon_i}$ are:

$$\frac{d\chi_1^+}{dt} = e^{-2\beta}\beta p_1(1 + p_1 + D) - e^{-2\beta}\chi_1^+(1 + 2p_1 + D) + D\chi_3^+, \quad (\text{C6})$$

$$\chi_3^+ = \frac{e^{-2\beta}}{1 + D} (\chi_1^+ D - \beta p_1(p_1 + D)), \quad (\text{C7})$$

$$\frac{d\chi_1^-}{dt} = e^{-2\beta}\beta p_1(p_0 + D) - e^{-2\beta}\chi_1^-(1 + 2p_1 + D) + D\chi_3^-, \quad (\text{C8})$$

$$\chi_3^- = \frac{e^{-2\beta}D}{1 + D} (\chi_1^- - \beta p_1). \quad (\text{C9})$$

From these equations we deduce closed linear differential equations for the response functions:

$$\frac{d\chi_1^+}{dt} = e^{-2\beta}\beta p_1 \left(1 + \frac{p_1 + D}{1 + D} \right) - e^{-2\beta}\chi_1^+ \left(1 + 2p_1 + \frac{D}{1 + D} \right), \quad (\text{C10})$$

$$\frac{d\chi_1^-}{dt} = e^{-2\beta}\beta p_1 \left(1 - p_1 + \frac{D}{1 + D} \right) - e^{-2\beta}\chi_1^- \left(1 + 2p_1 + \frac{D}{1 + D} \right). \quad (\text{C11})$$

For systems where all sites i are perturbed with uncorrelated ϵ_i , by self-averaging and linearity, the total response $\chi(t, t_w) \simeq \chi_1(t, t_w) = (\chi_1^+ + \chi_1^-)/2$ satisfies:

$$\frac{d\chi}{dt}(t, t_w) = - \left(1 + 2p_1(t) + \frac{D}{1 + D} \right) \chi(t, t_w) e^{-2\beta} + \beta p_1(t) \left(1 + \frac{D}{1 + D} - \frac{Dp_1(t)}{2(1 + D)} \right) e^{-2\beta}. \quad (\text{C12})$$

Discarding the third term in the last parenthesis allows us to solve this differential equation. This term may be neglected due to the small value of $p_1(t)$ for $t > t_w \gg D^{-1}$ or considering only the case of small diffusion constant D . Replacing $\chi(t, t_w) = \beta p_1(t)(\tilde{\chi}(t, t_w) + 1)$ leads to the following equation for $\tilde{\chi}$:

$$\frac{d\tilde{\chi}}{dt}(t, t_w) = - \frac{\tilde{\chi}(t, t_w)}{\tau_c} \quad (\text{C13})$$

with τ_c the timescale already introduced for the correlation function, Eq. (44), $\tau_c = e^{2\beta} [1 + D/(1 + D)]^{-1}$. A solution satisfying the initial condition $\chi(t_w, t_w) = 0$ or $\tilde{\chi}(t_w, t_w) = -1$ is:

$$\tilde{\chi}(t, t_w) = -e^{-(t-t_w)/\tau_c} \quad (\text{C14})$$

leading to the response function:

$$\chi^{(\text{MM})}(t, t_w) = \beta p_1(t) \left(1 - e^{-(t-t_w)/\tau_c} \right). \quad (\text{C15})$$

- [1] C.A. Angell, *Science* **267**, 1924 (1995).
- [2] M.D. Ediger, C.A. Angell and S.R. Nagel, *J. Phys. Chem.* **100**, 13200 (1996).
- [3] P.G. Debenedetti and F.H. Stillinger, *Nature* **410**, 259 (2001).
- [4] L. Santen and W. Krauth, *Nature* **405**, 550 (2000).
- [5] K.H. Fischer and J.A.Hertz, *Spin Glasses*, (Cambridge University Press, Cambridge, 1991).
- [6] A.P. Young (editor), *Spin-glasses and random fields*, (World Scientific, Singapore, 1997).
- [7] R.G. Palmer, D.L. Stein, E. Abraham, and P.W. Anderson, *Phys. Rev. Lett.* **53**, 958 (1984).
- [8] G.H. Fredrickson and H.C. Andersen, *Phys. Rev. Lett.* **53**, 1244 (1984).
- [9] See, eg., J. Jäckle and S. Eisinger, *Z. Phys.* **B84**, 115 (1991); Kob W and Andersen H C 1993 *Phys. Rev. E* **48** 4364; J. Kurchan, L. Peliti and M. Sellito, *Europhys. Lett.* **39**, 365 (1997); M. Schulz and S. Trimper, *J. Stat. Phys.* **94** 173 (1999); P. Sollich and M.R. Evans, *Phys. Rev. Lett.* **83**, 3238 (1999); J.P. Garrahan and M.E.J. Newman, *Phys. Rev. E* **62**, 7670 (2000); A. Barrat, J. Kurchan, V. Loreto and M. Sellitto, *Phys. Rev. Lett.* **85**, 5034 (2000); A. Crisanti, F. Ritort, A. Rocco and M. Sellitto, *J. Chem. Phys.* **113** 10615 (2001); A. Buhot and J.P. Garrahan, *Phys. Rev. E* **64**, 21505 (2001).
- [10] See papers in *J. Phys. Condens. Matter* **14**, 1381–1696 (2002), and references therein.

- [11] T. Aste and D. Sherrington, *J. Phys. A* **32**, 7049 (1999).
- [12] L. Davison and D. Sherrington, *J. Phys. A* **33** 8615 (2000).
- [13] L. Davison, D. Sherrington, J.P. Garrahan and A. Buhot, *J. Phys. A* **34**, 5147 (2001).
- [14] J. Cardy, *Field theory and non-equilibrium statistical mechanics*, Lectures presented as part of the Troisième Cycle de la Suisse Romande (1999), available at <http://www-thphys.physics.ox.ac.uk/users/JohnCardy/>.
- [15] H. Hinrichsen, *Adv. Phys.* **49**, 815 (2000).
- [16] We do not write explicitly the necessary sequence around the ‘Feynman diagram’ of the $T1$ process (see Fig. 1).
- [17] Processes (2) also lead to a one-site diffusion of the A or \bar{A} which remains after the annihilation.
- [18] The original model can also be described in terms of “spins” $q_i = 6 - n_i$, which are conventionally called “topological charges”.
- [19] The Abelian nature of the lattice-based dynamics, as opposed to the non-Abelian character of the foam, appears to be irrelevant to dominant order.
- [20] The annihilation of two dimers [process (1)] and its reverse process, which are not essential for the macroscopic dynamical behaviour, are not considered in this minimalist model.
- [21] F. Ritort, *Phys. Rev. Lett.* **75**, 1190 (1995).
- [22] C. Godrèche and J.M. Luck, *Eur. Phys. J. B* **23**, 473 (2001).
- [23] M.E.J. Newman and G.T. Barkema, *Monte Carlo Methods in Statistical Physics*, (OUP, Oxford, 1999).
- [24] A. Barrat, *Phys. Rev. E* **57**, 3629 (1998).
- [25] A. Buhot and J.P. Garrahan, *Phys. Rev. Lett.* **88**, 225702 (2002).
- [26] J.-P. Bouchaud, L.F. Cugliandolo, J. Kurchan and M. Mézard, in [6].
- [27] L. F. Cugliandolo, J. Kurchan and L. Peliti, *Phys. Rev. E* **55**, 3898 (1997).
- [28] M. Nicodemi, *Phys. Rev. Lett.* **82**, 3734 (1999).
- [29] A. Barrat and V. Loreto, *J. Phys. A* **33**, 4401 (2000).